Dinuclear Cobalt(II) Complexes of Pyrazole Ligands with Chelating Side Arms☆

Franc Meyer*, Stefan Beyreuther, Katja Heinze, and Laszlo Zsolnai

Anorganisch-Chemisches Institut der Universität Heidelberg,
Im Neuenheimer Feld 270, D-69120 Heidelberg, Germany
Fax: (internat.) +49(0)6221/54-5707
E-mail: Franc@sun0.urz.uni-heidelberg.de

Received November 4, 1996

Keywords: Pyrazolate complexes / Dinuclear complexes / Bridging ligands / Cobalt / Conformational analysis

A series of pyrazole-based potential ligands bearing polydentate amine substituents in the 3- and 5-positions of the heterocycle has been synthesized [3,5-bis(R_2NCH_2)-pyzH; R_2N = $Me_2N(CH_2)_3NMe$ (**2aH**), $\{Me_2N(CH_2)_3\}_2N$ (**2bH**), $(Et_2NCH_2CH_2)_2N$ (**2cH**)]. Upon reaction with two equivalents of $CoCl_2$ they form complexes LCo_2Cl_3 (**3a**–**c**; L = **2a**–**c**, respectively) which are shown crystallographically to contain a dinuclear metal core bridged by both the pyrazolate unit and a chlorine atom, with each cobalt center carrying a further terminal chlorine atom. Two of the ligand side arms in **3b**, **c** are dangling, thus leading to five-coordination of the cobalt(II) centers in all cases. Addition of two equivalents of $NaBPh_4$ to solutions of **3b**, **c** induced coordination of the formerly dangling side arms to the metal centers by substitution of the terminal chlorine atoms. The resulting compounds $[LCo_2Cl](BPh_4)_2$ (**4b**, **c**, respectively) were characterized by X-ray structure analyses. They can be viewed as dinuclear linked versions of tran-type complexes [(tran = tris(aminoalkyl)amine] with distorted trigonal-bipyramidal coordination spheres around cobalt(II). Conformational analyses employing force-field calculations were carried out for **4b**, **c** in order to rationalize the conformations observed in the solid state with regard to the accessible conformational space.

Introduction

There is considerable current interest in bi- and multimetallic transition metal complexes showing cooperative phenomena[1a,b]. A particular stimulus in this regard arises from the fact that many metallobiosites contain several metal ions in close proximity[1b]. In order to achieve distinct reactivity patterns based on the cooperation between two metal centers, the design of appropriate ligand cores providing coordination sites with well-defined metal-metal separations is essential[2], which justifies research concerning the synthesis and coordination potential of dinucleating systems.

The ability of the diazine unit of pyrazolates to bridge two metal ions is well known[3]. However, relatively few studies of dinuclear complexes of pyrazole-based ligands possessing additional chelating side arms in the 3- and 5-positions of the heterocycle have hitherto been reported[4–7]. Okawa and coworkers recently described a series of dimanganese complexes of pyrazoles carrying pyridyl or dialkylamino groups as pendant donors[7b]. These complexes exhibited catalytic activity towards the disproportionation of H_2O_2 and are thus regarded as interesting models for the dimanganese biosite of catalase.

Heterocyclic diazine groups as bridges in dinuclear complexes generally support metal-metal separations in the range of 3.4–4.5 Å, favorable for possible cooperativity. Based on this structural motif a fine-tuning of the particular steric and electronic requirements should be achievable by varying the chain lengths of the chelating substituents and the nature of the side-arm donor atoms, respectively (Scheme 1). In the present contribution we report the synthesis of a series of pyrazolate-based dinucleating ligands with pendant aliphatic dialkylamino groups (D1 = N, D2 = NR_2) having varying length of the side arms (x = 2, 3), Scheme 1. Making use of the great variety of accessible coordination geometries for the d^7 Co^{II} ion, complexes of these ligands with cobalt(II) chloride are studied in order to probe their coordination potential, and conformational analyses on the resulting compounds are carried out with a view to rationalize the observed solid-state structures and to ascertain the suitability of the applied force field for future ligand design.

Scheme 1

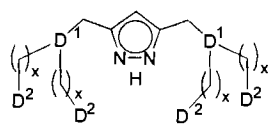

Results and Discussion

The synthesis of pyrazole-based ligands with pendant polyamino side arms was accomplished following a strategy described previously[7] (Scheme 2). Pyrazole-3,5-dicarboxylic acid was converted into amides **1aH**–**cH** by treatment with $SOCl_2$[5a] followed by reaction with the appropri-

  0009–2940/97/0505–0605 $ 17.50+.50/0

ate secondary amines in the presence of triethylamine. **1aH–cH** were then reduced with $LiAlH_4$ to yield the corresponding polydentate ligands **2aH–cH**, respectively, as slightly yellowish oils. Due to their polyamine functionalities, no suitable conditions for column chromatographic purification of **2aH–cH** could be found. However, the products obtained after the reduction step proved to be sufficiently pure for all subsequent complexation purposes.

Scheme 2

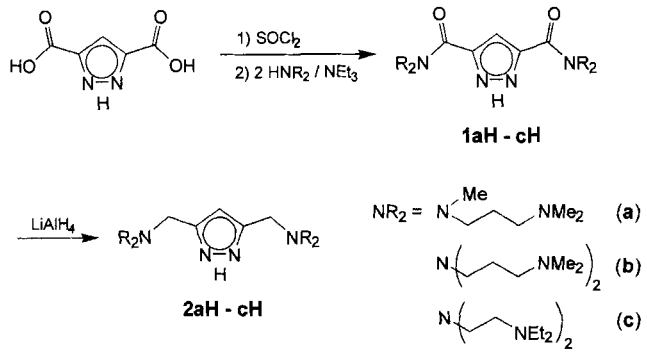

Synthesis and Characterization of Cobalt(II) Complexes

For the synthesis of cobalt complexes the potential ligands **2aH–cH**, respectively, were first deprotonated by treatment with BuLi. Subsequent addition of two equivalents of anhydrous $CoCl_2$ afforded solutions of the deep-blue complexes **2a** · Co_2Cl_3 (**3a**), **2b** · Co_2Cl_3 (**3b**), and **2c** · Co_2Cl_3 (**3c**), respectively. These could be crystallized by layering a solution in CH_2Cl_2 (**3b**) or THF (**3c**) with petroleum ether at −30 °C or by vapor diffusion of petroleum ether into a solution in $CHCl_3$ (**3a**) at room temp.

Formation of complexes of the type LCo_2Cl_3 (L = **2a–c**) was corroborated by elemental analyses and by the FAB-MS spectra. No definitive structural conclusions could be drawn from the solution UV/Vis/NIR data (Table 1), although the spectra resembled those observed for related mononuclear complexes such as (dienMe)$CoCl_2$ [dienMe = bis(2-dimethylaminoethyl)methylamine] containing five-coordinate high-spin Co^{II}[8]. The close similarity of the optical transition bands for compounds **3a–c** indicates an identical set of donor atoms and similar coordination geometry, thus suggesting that two of the side-arm nitrogen donors in **3b** and **3c** are non-coordinating.

Table 1. UV/Vis/NIR data of the complexes. $\tilde{\nu}$ in cm^{-1}, ε in M^{-1} cm^{-1}

3a	12240 (30), 15800 (181), 17450 (126), 18550 (113), 19530 (91)
3b	12150 (25), 15480 (129), 17510 (97), 18520 (95), 19570 (73)
3c	11850 (33), 16340 (209), 17210 (203), 18520 (sh, 132), 19490 (sh, 82)
4b	12600 (48), 17240 (146), 18550 (sh, 124), 19690 (sh, 100)
4c	12900 (45), 18080 (265), 19570 (sh, 171)

In order to unambiguously ascertain their coordination geometries, X-ray crystallographic analyses of complexes **3a–c** were carried out. Molecular structures are depicted in Figure 1.

All compounds show two cobalt atoms bridged by both a pyrazolate unit and a chlorine atom. The coordination sphere of each cobalt center further consists of two nitrogen donors from one side arm of the pyrazolate ligand and a terminal chlorine atom, thus resulting in pentacoordination. As concluded from the electronic absorption spectra, the two remaining amino groups in the dangling side arms of the ligands in complexes **3b, c** are non-coordinating. The coordination geometry around each cobalt atom can be described as being intermediate between distorted trigonal-bipyramidal and distorted square-pyramidal. The Co–N bond lengths lie in the range expected for high-spin Co^{II}, the shortest bonds being those to the pyrazolate-N (1.98–2.00 Å). The atom distances from Co to the branching N are significantly longer (2.28–2.33 Å), in accordance with the variations in bond lengths found for related mononuclear Co^{II} complexes, e.g. (dienMe)$CoCl_2$[9]. The μ-pyrazolate framework fixes the two metal centers with Co···Co separations of 3.913 Å (**3a**), 3.942 Å (**3b**), and 3.818 Å (**3c**), thus causing a slightly smaller distance in the case of **3c**, with the shorter side arms in the 3- and 5-positions of the heterocycle. A notable feature is the difference in relative configuration among the dinuclear complexes studied. While the coordinating pendant amino groups (and hence the dangling arms in **3b, c**) are each on the same side with respect to the μ-pyrazolato-dicobalt(II) core in **3a** and **3c**, they are located on different sides in **3b**. This results in an approximate (non-crystallographic) C_2 symmetry for **3b** and C_s symmetry for **3a, c**.

No ESR signals (*X*-band) of the polycrystalline powders could be detected at either room temp. or at 110 K for **3a–c**. Cyclic voltammograms of CH_2Cl_2 solutions of all complexes display an irreversible oxidation process in the range 1.0 to 1.2 V and an irreversible reduction wave at around −2.0 V vs. SCE.

Reaction of **3b, c** with two equivalents of $NaBPh_4$ in EtOH resulted in the immediate precipitation of light-purple complexes **4b, c**, respectively. Elemental analyses were in accordance with the formation of compounds of the type $[LCo_2Cl](BPh_4)_2$ (L = **2b, c**, respectively). **4b, c** were found to be stable in air, even over prolonged periods (weeks).

The solution UV/Vis/NIR spectral features (Table 1) bear close resemblance to previously reported band positions for pseudo-trigonal-bipyramidal high-spin cobalt(II) complexes containing tetradentate tripodal ligands[10,11]. A slight blue shift compared to the absorption bands of **3a–c** is observed for **4b, c**, in accord with a change of the donor set from N_3Cl_2 to N_4Cl.

X-ray structure determinations were carried out on single crystals obtained by vapor diffusion of Et_2O into acetonitrile solutions of the complexes. Molecular structures of the cations are depicted in Figure 2.

The basic structural feature of a (μ-pyrazolato)-(μ-chloro)-dicobalt(II) core found in **3b, c** is retained in **4b, c**.

Figure 1. Molecular structures of **3a** (top), **3b** (bottom left), and **3c** (bottom right); for clarity all hydrogen atoms have been omitted[a]

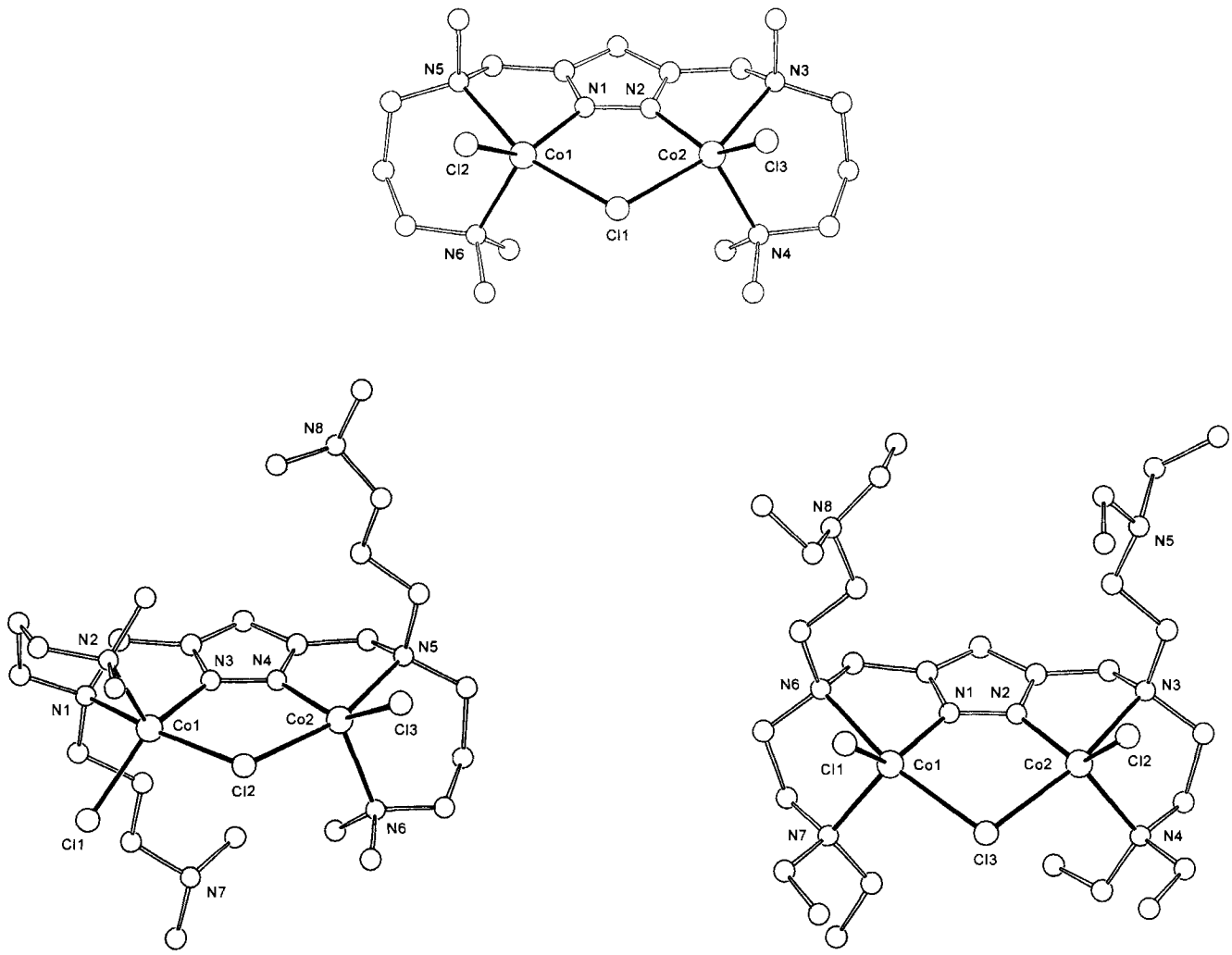

[a] Selected bond lengths [Å] and angles [°] (estimated standard deviations in parentheses): **3a**: Co1–N1 1.989(5), Co1–N5 2.301(6), Co1–N6 2.116(6), Co1–Cl1 2.454(2), Co1–Cl2 2.292(2), N1–N2 1.350(7); N1–Co1–N5 76.1(2), N1–Co1–N6 114.7(2), N1–Co1–Cl1 87.0(2), N1–Co1–Cl2 142.1(2), N6–Co1–N5 91.5(2), N5–Co1–Cl1 162.3(1), N5–Co1–Cl2 94.1(1), N6–Co1–Cl1 100.5(2), N6–Co1–Cl2 101.9(2), Cl1–Co1–Cl2 96.1(1), Co1–Cl1–Co2 105.1(1). – **3b**: Co1–N1 2.298(2), Co1–N2 2.113(2), Co1–N3 1.998(2), Co1–Cl1 2.301(1), Co1–Cl2 2.447(1), N3–N4 1.369(3); N1–Co1–N2 94.2(1), N1–Co1–N3 76.4(1), N1–Co1–Cl1 91.3(1), N1–Co1–Cl2 161.0(1), N2–Co1–N3 109.1(1), N2–Co1–Cl1 102.8(1), N2–Co1–Cl2 100.9(1), N3–Co1–Cl1 146.5(1), N3–Co1–Cl2 87.7(1), Cl1–Co1–Cl2 96.5(1), Co1–Cl2–Co2 105.4(1). – **3c**: Co1–N1 1.993(7), Co1–N6 2.328(8), Co1–N7 2.159(7), Co1–Cl1 2.289(3), Co1–Cl3 2.471(2), N1–N2 1.359(9); N1–Co1–N6 75.2(3), N1–Co1–N7 114.4(3), N1–Co1–Cl1 134.4(2), N1–Co1–Cl3 88.8(2), N6–Co1–N7 82.3(3), N6–Co1–Cl1 93.3(2), N6–Co1–Cl3 163.6(2), N7–Co1–Cl1 107.3(2), N7–Co1–Cl3 101.7(2), Cl1–Co1–Cl2 100.5(1), Co1–Cl3–Co2 101.4(1).

However, the formerly dangling arms are now coordinated to the metal centers due to substitution of the terminal chlorine atoms in **3b**, **c**. The coordination geometry around each cobalt center is distorted trigonal-bipyramidal, with the bridging Cl and the branching N (N3/N6 in **4b**, N3/N7 in **4c**) occupying the axial positions. All bond lengths are very similar to the corresponding values in the precursor complexes **3b**, **c**, respectively, as are the Co···Co separations (**4b**: 3.909 Å; **4c**: 3.833 Å). Again, the distance between the two metal atoms is slightly smaller in the case of the pyrazolate ligand with shorter side arms, i.e. **4c**. Compounds **4b**, **c** can be viewed as linked versions of the well-known mononuclear pentacoordinate Co^{II} complexes $[LCoCl]^+$, where L is a tripodal tetramine tran-type ligand [tran = tris(aminoalkyl)amine, e.g. tren = tris(2-aminoethyl)amine] in which one of the pendant amino groups is replaced by a bridging pyrazolate. The class of tetradentate ligands derived from tran has been shown to commonly enforce the adoption of trigonal-bipyramidal coordination in most complexes of M^{II} ions, with the additional monodentate ligand occupying an axial position[11]. In the present dinuclear case, the rigid pyrazolate framework forces this ad-

Figure 2. Molecular structure of the cations of **4b** (top) and **4c** (bottom); for clarity all hydrogen atoms have been omitted[a]

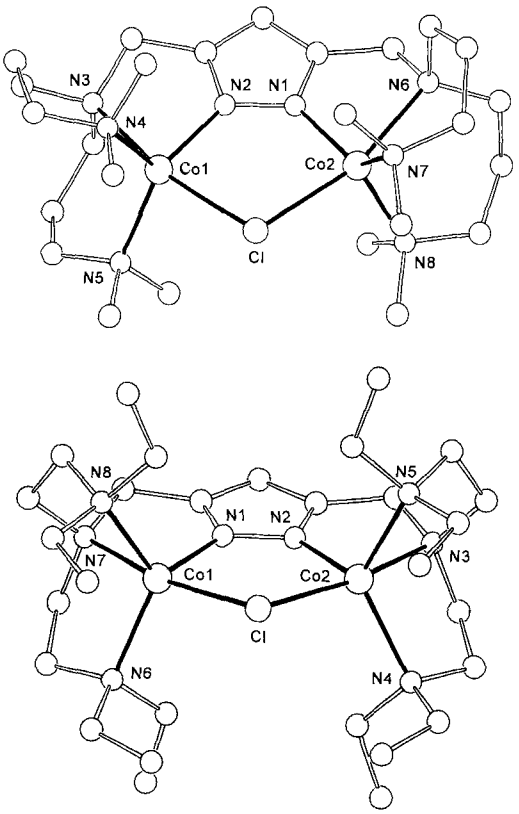

[a] Selected bond lengths [Å] and angles [°] (estimated standard deviations in parentheses): **4b**: Co1–N2 1.956(7), Co1–N3 2.324(8), Co1–N4 2.091(8), Co1–N5 2.089(8), Co1–Cl 2.465(3), N1–N2 1.377(9); N2–Co1–N3 77.3(3), N2–Co1–N4 112.6(3), N2–Co1–N5 129.9(3), N2–Co1–Cl 87.3(2), N3–Co1–N4 89.9(3), N3–Co1–N5 92.0(3), N3–Co1–Cl 162.8(2), N4–Co1–N5 116.2(3), N4–Co1–Cl 103.3(2), N5–Co1–Cl 92.0(2), Co1–Cl–Co2 104.79(9). – **4c**: Co1–N1 1.971(5), Co1–N6 2.114(5), Co1–N7 2.252(5), Co1–N8 2.106(5), Co1–Cl 2.449(2), N1–N2 1.367(6); N1–Co1–N6 116.0(2), N1–Co1–N7 77.2(2), N1–Co1–N8 115.1(2), N1–Co1–Cl 88.7(2), N6–Co1–N7 82.3(2), N6–Co1–N8 121.3(2), N6–Co1–Cl 105.4(2), N7–Co1–N8 82.6(2), N7–Co1–Cl 165.9(2), N8–Co1–Cl 102.7(2), Co1–Cl–Co2 103.9(1).

ditional ligand, i.e. Cl, to lie in a position spanning the two metal centers. Experiments aimed at replacing the bridging chlorine atom in **4b**, **c** by other inorganic and organic moieties are currently underway.

As for **3a–c**, no ESR signals (*X*-band) of the polycrystalline powders could be detected at either room temp. or at 110 K for **4b**, **c**. Magnetic susceptibility measurements on a dried, powdered sample of **4c** revealed Curie-Weiss law behavior in the temperature range 100–300 K (linear regression yields Θ = 15.2 K). The magnetic moment of 3.99 ± 0.02 μ_B per cobalt atom is close to the spin-only value for an S = 3/2 situation (3.87 μ_B). This is significantly smaller than the moments commonly observed for OC-6 cobalt(II) (4.7–5.3 μ_B) or T-4 cobalt(II) (4.2–4.8 μ_B)[12] and indicates that orbital angular momentum contributions are largely quenched in the present ligand field of low symmetry. Mononuclear trigonal-bipyramidal high-spin Co^{II} complexes with an N_4Cl donor set have been shown to exhibit magnetic moments in the range 4.2–4.5 μ_B[13]. Cyclic voltammograms of CH_3CN solutions of both complexes **4b**, **c** display an irreversible oxidation process at E_p^{ox} = 0.96 V vs. SCE, which reflects the fact that substituted tran-type ligands generally do not adapt to octahedral coordination as preferred for low spin Co^{III}.

Conformational Analyses

Corresponding to the differences in relative configuration observed for **3b**, **c** the dinuclear cations of **4b**, **c** show approximate (non-crystallographic) C_2 and C_s symmetries, respectively, in the solid state. In order to rationalize these conformations with respect to the accessible conformational space we performed conformational analyses applying force-field calculations on **4b**, **c**.

In a mononuclear tren-type system each torsional skew along the Co–N_{ax} bond corresponds to a preferred chelate ring conformation, namely combinations Δ/λ and Λ/δ. Mismatch between torsional skew and chelate conformation, i.e. combinations Δ/δ and Λ/λ, forces the five-membered ring to distort towards an envelope-like conformation with a torsion angle (C–N_{ax}–Co–N_{eq}) of almost 0° (Figure 3).

Figure 3

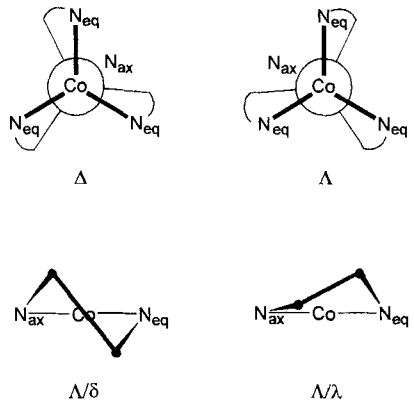

The rigid pyrazolate framework in **4c** restricts those five-membered chelates annellated to the pyrazolate to one conformation for a given torsional skew of the corresponding tren moiety, namely combinations Δ/λ and Λ/δ, respectively. The overall conformation is then described by a code of the type Δ(I II)Λ(III IV), where the first and second parts of the expression correspond to the Co1 and Co2 subunits, respectively, and the sequence of the descriptors in brackets follows the ordering as depicted in Figure 4, i.e. Δ(λλ)Λ(δδ) coding the X-ray crystal structure of **4c**.

A total number of 36 different stereoisomeric combinations of idealized ring conformations exist for the present

Figure 4

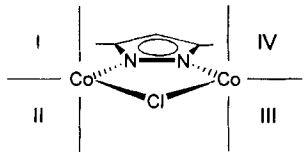

system **4c**[14]. Geometry optimization produced eight different diastereomeric local minimum structures, Table 2.

Table 2. Conformational isomers of **4c**

	Stereoisomer	Relative energy [kJ mol^{-1}]
$\mathbf{4c_1}$	Δ(λλ)Δ(λλ)	0.0
$\mathbf{4c_2}$	Δ(λλ)Λ(δδ)	5.0
$\mathbf{4c_3}$	Δ(λδ)Δ(λλ)	16.8
$\mathbf{4c_4}$	Δ(δλ)Δ(λλ)	18.8
$\mathbf{4c_5}$	Δ(λλ)Λ(δλ)	23.6
$\mathbf{4c_6}$	Δ(λδ)Δ(δλ)	32.2
$\mathbf{4c_7}$	Δ(λδ)Δ(λδ)	37.1
$\mathbf{4c_8}$	Δ(δλ)Δ(δλ)	37.2

The conformation Δ(λλ)Λ(δδ) observed for **4c** in the solid state was confirmed as the second lowest minimum, only 5 kJ/mol above the global minimum, i.e. Δ(λλ)Δ(λλ). These two species are those with an overall match (Δ/λ and Λ/δ, see above) between ring conformations and the corresponding torsional skew. All other conformational isomers contain at least one mismatch combination, i.e. Δ/δ or Λ/λ, and are thus significantly higher in energy (Table 2). Obviously, the change of a single chelate ring conformation, i.e. $\mathbf{4c_1}$ versus $\mathbf{4c_3}$, is accompanied by a considerable difference in terms of energy, while species differing by the inversion of a complete tren-type subunit, i.e. $\mathbf{4c_1}$ versus $\mathbf{4c_2}$, are very close in energy. Furthermore, it turns out that the introduction of a mismatch combination is favored in specific segments for a given torsional skew, that is, in segments II/IV in the case of Δ and in segments I/III for Λ, as reflected by the energetic difference between $\mathbf{4c_3}$ and $\mathbf{4c_4}$ compared to $\mathbf{4c_1}$.

It should be noted that replacement of the bridging chlorine atom in **4c** by two non-bridging ligands will strongly favor isomers of the type ΔΔ (or ΛΛ), because this allows those terminal ligands to lie on different sides with respect to the plane defined by the pyrazolate. Although the solid-state structure of **4c** displays the opposite type ΔΛ, stereoisomers of the appropriate type ΔΔ (or ΛΛ) should be easily adopted based on the present conformation analysis.

Similar considerations for **4b** reveal a more complicated situation due to the six-membered chelate rings, where torsional skews Δ and Λ combine with four pairs of chair (d/l) and twist-boat (λ_1/δ_1, δ_2/λ_2, λ_3/δ_3) conformations (Figure 5)[15]. However, the match/mismatch criterion now is an excluding restriction, allowing only one specific chair conformation and three different twist-boat conformations for a six-membered ring, depending on the corresponding torsional skew (Figure 5).

Figure 5

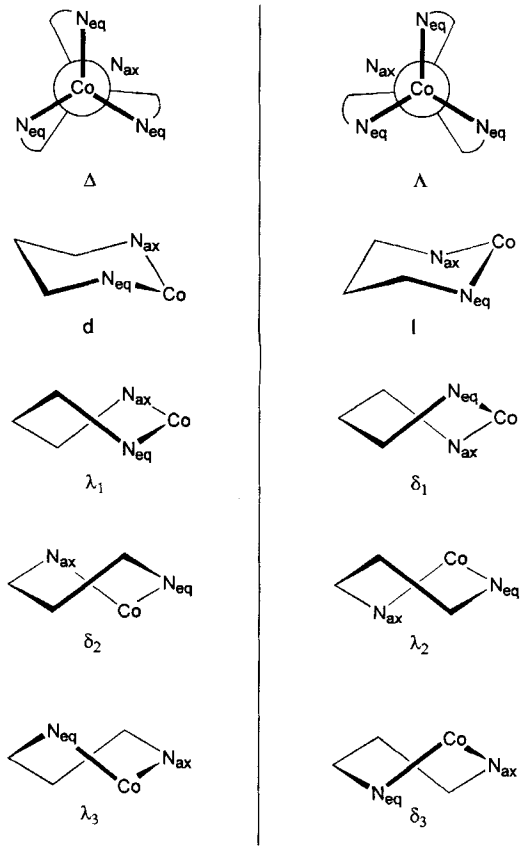

272 different diastereoisomeric combinations of idealized conformations are possible for **4b**[16]. In most cases, the given torsional skews of the starting configurations were preserved during geometry optimization, although changes in ring conformations did occur. The resulting seven different diastereomers of lowest energy are summarized in Table 3, together with few selected species of higher energy.

Table 3. Selected conformational isomers of **4b**

	Stereoisomer	Relative energy [kJ mol^{-1}]
$\mathbf{4b_1}$	Δ(dλ$_1$)Δ(dλ$_1$)	0.0
$\mathbf{4b_2}$	Δ(dλ$_1$)Δ(dd)	2.8
$\mathbf{4b_3}$	Λ(ll)Δ(dλ$_1$)	4.6
$\mathbf{4b_4}$	Λ(δ$_1$l)Δ(dd)	4.6
$\mathbf{4b_5}$	Δ(dd)Δ(dd)	6.5
$\mathbf{4b_6}$	Λ(δ$_1$l)Δ(dλ$_1$)	9.5
$\mathbf{4b_7}$	Λ(δ$_1$δ$_1$)Δ(dd)	14.1
.....	.....	.....
$\mathbf{4b_i}$	Δ(λ$_1$d)Δ(dλ$_1$)	26.3
.....	.....	.....
$\mathbf{4b_j}$	Δ(λ$_1$d)Δ(λ$_3$δ$_2$)	74.4
.....	.....	.....

The conformation $\Delta(d\lambda_1)\Delta(d\lambda_1)$, coding the structure observed for **4b** in the solid state, proved to be the global minimum of the conformational space. Within a range of 10 kJ/mol therefrom, conformations differing by the following features compared to the global minimum structure were found: *a)* one or even both λ_1 twist-boat rings also exhibiting chair conformations (**4b$_2$** and **4b$_5$**, respectively); or *b)* inversion of a complete subunit [$\Delta(d\lambda_1)$ versus $\Lambda(\delta_1 l)$, **4b$_6$**], or *c)* a possible combination of both a) and b) (**4b$_3$** and **4b$_4$**, respectively). Obviously, the chair and λ_1/δ_1 twist-boat are the preferred conformations for the six-membered chelate rings. In addition, the two Co1- and Co2-subunits are essentially decoupled, thus causing only a small difference in energy if a whole subunit displays complete inversion. Twist-boat conformations δ_2 and λ_2, respectively, appear to be very unfavorable and only occur for species lying at least 20 kJ/mol above the global minimum. This is because the torsional skew along the Co–N_{ax} axis for Δ (Λ) is restricted to angles $<36°$ ($>-36°$) by the five-membered ring annellated to the pyrazolate, which is incompatible with the torsion angles of around 65° (−65°) required for δ_2 (λ_2). Unsymmetrical twist-boats λ_3 (δ_3) turned out to be less favored as compared to λ_1 (δ_1) due to a more severe distortion of the twist-boat ring in the former case. This distortion arises from the fact that the "crossing" bonds in the chelate ring (Figure 5) differ significantly in the λ_3 (δ_3) situation, being a long Co–N_{eq} and a short C–C bond. Finally, preferred overall structures are not only determined by the type of individual chelate ring conformations, but also by their relative positions, e.g. $\Delta(d\lambda_1)$ and $\Lambda(\delta_1 l)$ being considerably favored over $\Delta(\lambda_1 d)$ and $\Lambda(l\delta_1)$, respectively (**4b$_1$** versus **4b$_i$**), due to specific interactions between the substituents at nitrogen.

Summary

In conclusion, the present series of pyrazolate-derived polydentate N-donor ligands was proven to give rise to dinuclear complexes, inducing five-coordination at the metal centers with the remaining coordination site in a dinucleating bridging position. Conformational analyses confirmed the conformations observed for the solid-state structures of **4b**, **c** as the global or second lowest minimum of the respective conformational space. This result ascertains that the conformations found in the solid state are mainly governed by internal forces and that the applied force field is a suitable tool for future ligand design based on observed X-ray crystal structures. It furthermore corroborates[15] that it is a reasonable approach to generate all probable idealized structures individually and to minimize them separately in order to determine the global minimum conformation of complexes of this nature. For the compounds studied, certain conformations are favored within a tran-type coordination sphere, while the two subunits of the complexes **4b**, **c** are largely decoupled. This leaves both complexes with a significant amount of conformational freedom, which should allow them to adapt to other moieties in place of the bridging chlorine atom. Of particular interest in this context is the replacement of the chlorine by two terminal ligands that require conformations of the type $\Delta\Delta$ ($\Lambda\Lambda$). Work in this area is presently in progress.

We thank Prof. Dr. *G. Huttner* for his generous support of our work as well as the *Fonds der Chemischen Industrie* for providing a Liebig-Stipendium (to F. M.).

Experimental Section

All manipulations were carried out under an atmosphere of dry nitrogen by employing standard Schlenk techniques. Solvents were dried according to established procedures. Compounds **1a–c**, **2a–c** were prepared following a strategy already described for **2c**[7a]. – Microanalyses: Mikroanalytische Laboratorien des Organisch-Chemischen Instituts der Universität Heidelberg. – IR spectra: Bruker IFS 66 FTIR. – ^{1}H and ^{13}C{^{1}H} NMR spectra: Bruker AC 200 at 200.13 MHz and 50.32 MHz, respectively. Signal of the solvent as chemical shift reference. $CDCl_3$: δ_H = 7.27, δ_C = 77.0; [D_6]DMSO: δ_H = 2.50, δ_C = 39.5. – MS (FAB and EI) spectra: Finnigan MAT 8230. – UV/Vis/NIR spectra: Perkin-Elmer Lambda 19. – ESR spectra: Bruker ESP 300 E, *X*-band, external standard DPPH, temperature control unit Eurotherm B-VT 2000. – Cyclic voltammetry: PAR equipment (potentiostat/galvanostat 273), 10^{-3} M in 0.1 M *n*Bu_4NPF_6/CH_3CN (**4b**, **c**) or in 0.1 M *n*-Bu_4NPF_6/CH_2Cl_2 (**3a–c**), respectively. Potentials in V on glassy carbon electrode, referenced to saturated calomel electrode (SCE) at ambient temperature. – Magnetic measurements: Bruker Magnet B-E 15 C8, field-controller B-H 15, variable temperature unit ER4111VT, Sartorius micro balance M 25 D-S.

3,5-Bis{N-[3-(dimethylamino)propyl]-N-methylcarbamoyl}-pyrazole (**1a**): Pyrazole-3,5-dicarboxylic acid monohydrate (3.3 g, 19.0 mmol) was converted into 3,5-bis(chloroformyl)pyrazole by treatment with $SOCl_2$[5a]. This was taken up in 150 ml of THF and a solution of 1-(dimethylamino)-3-(methylamino)propane (5.9 ml, 40.3 mmol) and triethylamine (9.0 ml, 64.9 mmol) in 150 ml of THF was added dropwise with stirring. The reaction mixture was left at room temp. overnight, then filtered and concentrated to dryness. The resulting crude oil was redissolved in 40 ml of THF and filtered once more. After removal of all volatile material in vacuo, 5.7 g (85%) of the product remained as a white solid. – ^{1}H NMR ($CDCl_3$): δ = 1.87 (m, 4H, CH_2), 2.27 (s, 12H, CH_3), 2.33 (m, 4H, CH_2), 3.05, 3.27 [2 s, 4H, (*E*/*Z*)-$CONCH_3$], 3.64 (m, 4H, $CONCH_2$), 7.02 (s, 1H, pyrazole-H^4). – ^{13}C{^{1}H} NMR ($CDCl_3$): δ = 24.8, 25.6 (CH_2), 33.2, 33.5, 37.5, 44.8, 45.1, 45.8 (CH_3), 47.1, 47.9, 48.6, 54.6, 55.5, 57.3 (CH_2), 110.8, 111.0 (pyrazole-C^4), 140.4, 142.9, 145.8 (br., pyrazole-C$^{3/5}$), 162.9, 163.7 (CO). – MS (FAB); *m/z* (%): 353 (100) [M^+ + 1], 308 (36) [M^+ − NMe_2]. – $C_{17}H_{32}N_6O_2$ (352.5): calcd. C 57.93, H 9.15, N 23.84; found C 57.01, H 8.94, N 23.12.

3,5-Bis{N,N-di[3-(dimethylamino)propyl]carbamoyl}pyrazole (**1b**): Starting from pyrazole-3,5-dicarboxylic acid monohydrate (4.2 g, 24.1 mmol), bis[3-(dimethyl-amino)propyl]amine (11.6 ml, 52.1 mmol), and triethylamine (8.5 ml, 61.3 mmol), the preparation was carried out analogously to that of **1a** to yield 9.9 g (83%) of the product as a slightly yellow oil. – ^{1}H NMR ($CDCl_3$): δ = 1.78 (br. m, 8H, CH_2), 2.17, 2.18 (2 s, 24H, CH_3), 2.28 (t, *J* = 6.9 Hz, 8H, Me_2NCH_2), 3.42 (t, *J* = 7.4 Hz, 4H, $CONCH_2$), 3.58 (t, *J* = 7.4 Hz, 4H, $CONCH_2$), 6.97 (s, 1H, pyrazole-H^4). – ^{13}C{^{1}H} NMR ($CDCl_3$): δ = 25.0 (CH_2), 25.5 (CH_2), 43.8 (Me_2NCH_2), 44.6 (CH_3), 45.1 (CH_3), 45.9 (Me_2NCH_2), 55.1 ($CONCH_2$), 56.8

($CONCH_2$), 110.7 (pyrazole-C^4), 142.6 (br., pyrazole-$C^{3/5}$), 162.5 (CO). – MS (FAB); *m/z* (%): 495 (100) [M^+ + 1]. – $C_{25}H_{50}N_8O_2$ (494.7): calcd. C 60.70, H 10.19, N 22.65; found C 59.73, H 10.03, N 20.77. No satisfactory analytical data (N percentage) could be obtained for this compound.

3,5-Bis{N,N-bis[2-(diethylamino)ethyl]carbamoyl}pyrazole[7a] (**1c**): Starting from pyrazole-3,5-dicarboxylic acid monohydrate (2.8 g, 16.1 mmol), *N,N,N',N'*-tetraethyldiethylenetriamine (8.5 ml, 33.1 mmol), and triethylamine (5.0 ml, 36.1 mmol), the preparation was carried out analogously to that of **1a** to yield 7.6 g (86%) of the product as a slight yellow oil. – ^1H NMR ($CDCl_3$): δ = 1.05 (t, *J* = 7.0 Hz, 24H, CH_3), 2.60 (quint, *J* = 7.0 Hz, 16H, CH_2), 2.74 (t, *J* = 6.8 Hz, 8H, CH_2), 3.54 (t, *J* = 6.8 Hz, 4H, $CONCH_2$), 3.72 (t, *J* = 6.8 Hz, 4H, $CONCH_2$), 7.09 (s, 1H, pyrazole-H^4). – $^{13}C\{^1H\}$ NMR ($CDCl_3$): δ = 11.5 (CH_2), 11.7 (CH_2), 45.1 (CH_2), 47.5 (CH_3), 48.0 (CH_3), 48.4 (CH_2), 50.1 ($CONCH_2$), 51.8 ($CONCH_2$), 111.2 (pyrazole-C^4), 162.6 (CO). – MS (FAB); *m/z* (%): 551 (100) [M^+ + 1]. – $C_{29}H_{58}N_8O_2$ (550.8): calcd. C 63.24, H 10.61, N 20.34; found C 61.50, H 10.48, N 19.45. No satisfactory analytical data (C percentage) could be obtained for this compound.

3,5-Bis{[N-(3-dimethylamino)propyl-N-methyl]aminomethyl}-pyrazole (**2a**): A solution of **1a** (5.7 g, 16.2 mmol) in 100 ml of THF was added dropwise to a stirred suspension of $LiAlH_4$ (2.0 g, 52.7 mmol) in 200 ml of THF. After completion of the addition, the reaction mixture was heated to reflux for 12 h and then, while cooling to 0°C, was carefully quenched with 10 ml of water. All inorganic precipitates were separated by filtration and washed with two 50 ml portions of THF. The combined filtrates were concentrated to dryness and the crude residual oil was redissolved in 50 ml of petroleum ether 40/60 and filtered once more. Evaporation of all volatile materials in vacuo afforded 3.7 g (70%) of the product as a slightly yellow oil. – ^1H NMR ($CDCl_3$): δ = 1.65 (quint, *J* = 7.0 Hz, 4H, CH_2), 2.22 (s, 18H, CH_3), 2.27 (t, *J* = 7.0 Hz, 4H, CH_2), 2.38 (t, *J* = 7.0 Hz, 4H, CH_2), 3.55 (s, 4H, CH_2), 5.97 (s, 1H, pyrazole-H^4). – $^{13}C\{^1H\}$ NMR ($CDCl_3$): δ = 25.4 (CH_2), 42.8 (CH_3), 45.6 (CH_3), 54.8 (br., CH_2), 57.6 (br., CH_2), 103.4 (pyrazole-C^4). – MS (FAB); *m/z* (%): 325 (98) [M^+ + 1], 209 (100) [$M^+ - C_6H_{16}N_2$]. – $C_{17}H_{36}N_6$ (324.5): calcd. C 62.92, H 11.18, N 25.90; found C 62.30, H 11.83, N 24.57.

3,5-Bis{N,N-bis[3-(dimethylamino)propyl]aminomethyl}pyrazole (**2b**): Starting from **1b** (6.4 g, 12.9 mmol) and $LiAlH_4$ (1.7 g, 44.8 mmol), the preparation was carried out analogously to that of **2a** to yield 4.1 g (68%) of the product as a colourless oil. – IR (film): $\tilde{\nu}$ = 3184 cm^{-1} (m), 2943 (s), 2813 (s), 1460 (s), 1040 (m). – ^1H NMR ($CDCl_3$): δ = 1.63 (quint, *J* = 7.1 Hz, 8H, CH_2), 2.21 (s, 24H, CH_3), 2.28 (t, *J* = 7.1 Hz, 8H, NCH_2), 2.46 (t, *J* = 7.1 Hz, 8H, NCH_2), 3.63 (s, 4H, CH_2), 5.92 (s, 1H, pyrazole-H^4). – $^{13}C\{^1H\}$ NMR ([D_6]DMSO): δ = 24.8 (CH_2), 45.2 (CH_3), 49.6 (br., CH_2), 51.2 (CH_2), 57.2 (CH_2), 103.7 (pyrazole-C^4). – MS (FAB); *m/z* (%): 467 (100) [M^+ + 1]. – $C_{25}H_{54}N_8$ (466.8): calcd. C 64.33, H 11.66, N 24.01; found C 63.17, H 11.43, N 23.66.

3,5-Bis{N,N-bis[2-(diethylamino)ethyl]aminomethyl}pyrazole[7a] (**2c**): Starting from **1c** (7.6 g, 13.8 mmol) and $LiAlH_4$ (1.8 g, 47.4 mmol), the preparation was carried out analogously to that of **2a** to yield 5.4 g (75%) of the product as a colourless oil. – IR (film): $\tilde{\nu}$ = 3182 cm^{-1} (m), 2971 (s), 2806 (s), 1468 (s), 1383 (s), 1069 (s). – ^1H NMR ($CDCl_3$): δ = 1.01 (t, *J* = 7.1 Hz, 24H, CH_3), 2.54 (quint, *J* = 7.1 Hz, 16H, CH_2CH_3), 2.58 (m, 16H, CH_2CH_2), 3.70 (s, 4H, CH_2), 5.92 (s, 1H, pyrazole-H^4). – $^{13}C\{^1H\}$ NMR ($CDCl_3$): δ = 11.3 (CH_3), 47.2 (CH_2CH_3), 49.6 (br., CH_2), 51.0 (br., CH_2), 51.5 (br., CH_2), 52.3 (br., CH_2), 53.5 (br., CH_2), 101.5 (pyrazole-C^4). – MS (EI); *m/z* (%): 522 (22) [M^+], 436 (84) [$M^+ - CH_2NEt_2$], 86 (100) [$CH_2NEt_2^+$]. – $C_{29}H_{62}N_8$ (522.9): calcd. C 66.62, H 11.95, N 21.43; found C 65.74, H 11.87, N 21.00.

μ-Chloro-μ-{3,5-bis{[N-(3-dimethylamino)propyl-N-methyl]-aminomethyl}pyrazolate}dicobalt(II) Dichloride (**3a**): A solution of **2a** (0.18 g, 0.55 mmol) in 20 ml of THF was treated with one equivalent of BuLi (2.5 M in hexane) and stirred for 15 min at room temp. Anhydrous $CoCl_2$ (0.14 g, 1.08 mmol) was then added in one portion and the reaction mixture was stirred for a further 1 h. After evaporation of the solvent, the solid residue was taken up in CH_2Cl_2 (20 ml), undissolved material was filtered off and all volatile compounds were removed in vacuo. Purple-blue crystals of **3a** · 2 $CHCl_3$ (0.32 g, 74%) were obtained by vapor diffusion of petroleum ether 40/60 into a $CHCl_3$ solution. – IR (KBr): $\tilde{\nu}$ = 3001 cm^{-1} (m), 1522 (m), 1469 (s), 1313 (s), 1036 (s), 826 (s). – MS (FAB); *m/z* (%): 512 (100) [M^+ – Cl]. – $C_{17}H_{35}Cl_3Co_2N_6$ (547.7): calcd. C 37.28, H 6.44, N 15.34; found C 36.73, H 6.49, N 14.88.

μ-Chloro-μ-{3,5-bis{N,N-di[3-(dimethylamino)propyl]-aminomethyl}pyrazolate}dicobalt(II) Dichloride (**3b**): Starting from **2b** (0.27 g, 0.58 mmol) and $CoCl_2$ (0.15 g, 1.16 mmol), the preparation was carried out analogously to that of **3a**. Blue crystals of **3b** · 2 CH_2Cl_2 (0.36 g, 72%) were formed within 10 d when a solution in CH_2Cl_2 was overlayed with petroleum ether and stored at −30°C. – IR (film): $\tilde{\nu}$ = 2962 cm^{-1} (m), 1515 (w), 1466 (s), 1261 (m), 1042 (m), 801 (s). – MS (FAB); *m/z* (%): 654 (100) [M^+ – Cl]. – $C_{25}H_{53}Cl_3Co_2N_8$ · 2 CH_2Cl_2 (859.8): calcd. C 37.72, H 6.68, N 13.03, Cl 28.86; found C 38.17, H 6.73, N 13.14, Cl 28.21.

μ-Chloro-μ-{3,5-bis{N,N-di[2-(diethylamino)ethyl]-aminomethyl}pyrazolate}dicobalt(II) Dichloride (**3c**): Starting from **2c** (0.26 g, 0.50 mmol) and $CoCl_2$ (0.13 g, 1.00 mmol), the preparation was carried out analogously to that of **3a**. Purple-blue crystals of **3c** (0.32 g, 86%) were obtained within 10 d when a solution in THF was overlayed with petroleum ether 40/60 and stored at −30°C. – IR (KBr): $\tilde{\nu}$ = 2970 cm^{-1} (s), 1512 (m), 1470 (s), 1459 (s), 1259 (m), 1064 (s), 763 (s). – MS (FAB); *m/z* (%): 710 (100) [M^+ – Cl]. – $C_{29}H_{61}Cl_3Co_2N_8$ (746.1): calcd. C 46.69, H 8.24, N 15.02, Cl 14.25; found C 46.25, H 8.24, N 14.83, Cl 13.95.

μ-Chloro-μ{3,5-bis{N,N-di[3-(dimethylamino)propyl]-aminomethyl}pyrazolate}dicobalt(II) Bis(tetraphenylborate) (**4b**): To a solution of **3b** (0.31 g, 0.47 mmol) in 30 ml of ethanol was added $NaBPh_4$ (0.32 g, 0.94 mmol) in one portion, causing the immediate precipitation of complex **4b**. It was filtered off, washed twice with small portions of ethanol, and dried in vacuo to give 0.56 g (95%) of the crude product. Small violet crystals were obtained by layering a solution of the complex in acetonitrile with Et_2O at −30°C (0.31 g, 52%). – IR (KBr): $\tilde{\nu}$ = 3053 cm^{-1} (m), 1579 (m), 1479 (s), 1262 (m), 967 (m), 708 (s), 611 (s). – $C_{73}H_{93}B_2ClCo_2N_8$ (1257.5): calcd. C 69.72, H 7.45, N 8.91; found C 67.72, H 7.52, N 8.94. No satisfactory analytical data (C percentage) could be obtained for this compound.

μ-Chloro-μ-{3,5-bis{N,N-di[2-(diethylamino)ethyl]amino-methyl}pyrazolate}dicobalt(II) Bis(tetraphenylborate) (**4c**): Starting from **3c** (0.33 g, 0.46 mmol) and $NaBPh_4$ (0.32 g, 0.93 mmol), the preparation was carried out analogously to that of **3b**. The product could be crystallized by layering a solution in acetonitrile with Et_2O at −30°C, to yield 0.49 g (81%) of purple plates. – IR (KBr): $\tilde{\nu}$ = 3053 cm^{-1} (m), 1579 (m), 1478 (s), 1262 (m), 734 (s), 706 (s), 611 (s). – MS (FAB); *m/z* (%): 993 (10) [M^+ – BPh_4], 674 (74) [M^+ – 2 BPh_4], 337 (100) [M^{2+} – 2 BPh_4]. – $C_{77}H_{101}B_2ClCo_2N_8$ (1313.6): calcd. C 70.40, H 7.75, N 8.53; found C 70.10, H 8.17, N 8.75.

Table 4. Crystallographic data of compounds **3a**, **3b**, **3c**, **4b**, and **4c**

	3a	**3b**	**3c**	**4b**	**4c**
Formula	$C_{17}H_{35}Cl_3Co_2N_6 \cdot 2\,CHCl_3$	$C_{25}H_{53}Cl_3Co_2N_8 \cdot 2\,CH_2Cl_2$	$C_{29}H_{61}Cl_3Co_2N_6$	$C_{73}H_{93}B_2ClCo_2N_8$	$C_{77}H_{101}B_2ClCo_2N_8 \cdot 1.75\,CH_3CN$
M_r	786.5	859.8	746.1	1257.5	1385.4
crystal size [mm]	0.15 × 0.25 × 0.25	0.30 × 0.30 × 0.30	0.20 × 0.20 × 0.20	0.20 × 0.15 × 0.20	0.15 × 0.20 × 0.20
crystal system	orthorhombic	monoclinic	orthorhombic	triclinic	triclinic
space group	*P*bca	$P2_1/c$	*P*bca	$P\bar{1}$	$P\bar{1}$
a [Å]	25.924(4)	12.224(2)	23.025(5)	11.773(3)	13.482(3)
b [Å]	19.325(4)	19.898(4)	14.252(3)	14.750(4)	14.417(4)
c [Å]	13.149(3)	16.908(4)	24.042(4)	19.995(4)	21.854(3)
α [°]	90	90	90	100.48(2)	81.80(2)
β [°]	90	97.67(1)	90	99.80(2)	88.95(1)
γ [°]	90	90	90	101.00(2)	64.84(2)
V [Å^3]	6587(2)	4076(1)	7889(3)	3275(1)	3801(1)
$\rho_{calcd.}$ [g cm^{-3}]	1.586	1.401	1.222	1.273	1.210
Z	8	4	8	2	2
F(000) [e]	3200	1792	3008	1332	1477
T [K]	200	200	200	200	200
μ (Mo-K$_\alpha$) [mm^{-1}]	1.759	1.302	1.072	0.596	0.521
scan mode	ω	ω	ω	ω	ω
hkl range	−10/34, −15/25, ±17	−5/13, −3/21, ±18	−24/27, −9/16, −21/28	0/13, ±17, ±24	−12/14, ±16, ±25
2θ range [°]	4.1–52.0	4.1–46.0	3.4–50.0	3.6–52.0	3.8–48.0
measured refl.	6461	5991	6946	11387	12401
observed refl. $I>2\sigma(I)$	3454	4749	3239	5417	6668
refined parameters	355	421	378	693	853
resid. electron dens. [eÅ^{-3}]	0.739/−0.513	0.446/−0.461	0.510/−0.443	0.962/−0.875	0.988/−0.363
R1	0.068	0.032	0.082	0.099	0.072
wR2 (refinement on F^2)	0.159	0.084	0.212	0.311	0.197
Goodness-of-fit	1.170	1.167	1.035	1.491	1.028

Conformation Analyses: The force-field calculations were carried out using the molecular mechanics module Discover of the molecular modeling software package Insight II[17] on a Silicon Graphics workstation Indigo^2, MIPS R4400, 200 MHz, 64 MB RAM, 2 GB hard disk. The Extensible Systematic Force Field (ESFF) was used. The atom type for the cobalt atoms was set to trigonal-bipyramidal Co^{2+} (Co025t). All other atom types were set as assigned by the program. A molecular charge of +2 was applied to calculate the partial charges. The only force-field parameter modified was the force constant for the out-of-plane angle of the pyrazolate nitrogen (atom type np). It was set to the value for aromatic carbon (atom type cp) to reproduce the observed solid-state structures of **4b**, **c**. In the conformational analyses, each of the conformations investigated was first generated according to the corresponding code by restrained minimization starting from the X-ray crystal structure. This conformation then served as a starting geometry for the free minimization, resulting in a local minimum structure which was stored. The restrained minimizations applied 14 torsional restraints (quadratic form, force constant = 100.0 kcal/mol, maximum force = 1000.0 kJ/mol), two for each of the four coded chelate rings and three for each torsional skew Δ/Λ, and fixed the atoms of the pyrazolate and the two cobalt atoms. Both restrained/fixed and unrestrained/unfixed minimizations were carried out in three steps, first using steepest descent (convergence: maximum derivative = 10.0 kcal/Å · mol), then Polak-Ribière conjugate gradient (convergence: maximum derivative = 0.1 kcal/Å · mol) and finally Broyden-Fletcher-Goldfarb-Shanno (BFGS) Newton minimization (convergence: maximum derivative = 0.001 kcal/Å · mol). Parameters not specified explicitly were used as set by default.

X-ray Structure Determinations: The measurements were carried out on a Siemens P4 (Nicolet Syntex) R3m/v four-circle diffractometer with graphite-monochromated Mo-K_α radiation. All calculations were performed with a micro-vax computer using the SHELXT PLUS software package. Structures were solved by direct methods with the SHELXS-86 program and refined using SHELX93[18]. An absorption correction (ψ scan, Δψ = 10°) was applied to all data. Atomic coordinates and anisotropic thermal parameters of the nonhydrogen atoms were refined by full-matrix least-squares calculation. In the case of **3c**, the ethyl groups of the non-coordinating N5 and N8 were disordered and were thus refined isotropically and without hydrogen atoms. Due to the small size and moderate quality of their crystals, the structure analyses of **3c** and **4b** could only be refined to final (poor) agreement values of $R = 0.082$ and 0.099, respectively. Data for the structure determinations is compiled in Table 4. Further details of the crystal structure investigations are available from the Fachinformationszentrum Karlsruhe, D-76344 Eggenstein-Leopoldshafen (Germany), on quoting the depository numbers CSD-406505 (**3a**), -406504 (**3b**), -406502 (**3c**), -406503 (**4b**), and -406501 (**4c**), the names of the authors, and the journal citation.

☆ Dedicated to Prof. Dr. *Walter Siebert* on the occasion of his 60th birthday.

[1] [1a] G. Süss-Fink, *Angew. Chem.* **1994**, *106*, 71–73; *Angew. Chem. Int. Ed. Engl.* **1994**, *33*, 67–69; W.-J. Peng, S. G. Train, D. K. Howell, F. R. Fronczek, G. G. Stanley, *J. Chem. Soc., Chem. Commun.* **1996**, 2607–2608. – [1b] J. Reedijk, *Bioinorganic Catalysis*, Marcel Dekker, New York, **1993**; R. H. Holm, *Pure Appl. Chem.* **1995**, *67*, 217–224; H. Steinhagen, G. Helmchen, *Angew. Chem.* **1996**, *108*, 2489–2492; *Angew. Chem. Int. Ed. Engl.* **1996**, *35*, 2339–2342; N. Sträter, W. N. Lipscomb, T. Klabunde, B. Krebs, *Angew. Chem.* **1996**, *108*, 2158–2190; *Angew. Chem. Int. Ed. Engl.* **1996**, *35*, 2024–2055; K. D. Karlin, *Science* **1993**, *261*, 701–708.

[2] See for example: S. R. Collinson, D. E. Fenton, *Coord. Chem. Rev.* **1996**, *148*, 19–40; H. Okawa, H. Sakiyama, *Pure Appl. Chem.* **1995**, *67*, 273–280. L. Que, Jr., Y. Dong, *Acc. Chem.*

Res. **1996**, *29*, 190–196; D. Volkmer, A. Hörstmann, K. Griesar, W. Haase, B. Krebs, *Inorg. Chem.* **1996**, *35*, 1132–1135.
[3] P. J. Steel, *Coord. Chem. Rev.* **1990**, *106*, 227–265; A. P. Sadimenko, S. S. Basson, *ibid.* **1996**, *147*, 247–297.
[4] T. G. Schenck, J. M. Downes, C. R. C. Milne, P. B. Mackenzie, H. Boucher, J. Whelan, B. Bosnich, *Inorg. Chem.* **1985**, *24*, 2334–2337.
[5] [5a] C. Acerete, J. M. Bueno, L. Campayo, P. Navarro, M. I. Rodriguez-Franco, *Tetrahedron*, **1994**, *50*, 4765–4774. – [5b] M. Kumar, V. J. Aran, P. Navarro, A. Ramos-Gallardo, A. Vegas, *Tetrahedron. Lett.* **1994**, *35*, 5723–5726.
[6] L. Behle, M. Neuburger, M. Zehnder, T. A. Kaden, *Helv. Chim. Acta* **1995**, *78*, 693–702.
[7] [7a] T. Kamiusuki, H. Okawa, E. Kitaura, K. Inoue, S. Kida, *Inorg. Chim. Acta* **1991**, *179*, 139–143. – [7b] M. Itoh, K. Motoda, K. Shindo, T. Kamiusuki, H. Sakiyama, N. Matsumoto, H. Okawa, *J. Chem. Soc., Dalton Trans.* **1995**, 3635–3641 and references cited therein.
[8] M. Ciampolini, G. P. Speroni, *Inorg. Chem.* **1966**, *5*, 45–49.
[9] M. Di Vaira, P. L. Orioli, *J. Chem. Soc., Chem. Commun.* **1966**, 590; Z. Dori, R. Eisenberg, H. B. Gray, *Inorg. Chem.* **1967**, *3*, 483–486.
[10] M. Ciampolini, N. Nardi, *Inorg. Chem.* **1966**, *5*, 41–44; M. Ciampolini, N. Nardi, G. P. Speroni, *Coord. Chem. Rev.* **1966**, *1*, 222–233; C. Furlani, *ibid.* **1968**, *3*, 141–167.
[11] S. G. Zipp, A. P. Zipp, S. K. Madan, *Coord. Chem. Rev.* **1974**, *14*, 29–45.
[12] R. L. Carlin, *Trans. Met. Chem.* **1965**, *1*, 1–32.
[13] L. V. Interrante, J. L. Shafer, *Inorg. Nucl. Chem. Lett.* **1968**, *4*, 411–417; A. Dei, R. Morassi, *J. Chem. Soc. (A)* **1971**, 2024–2027; L. Sacconi, *Coord. Chem. Rev.* **1972**, *8*, 351–367.
[14] The ten different species ΔΔ (four of which are C_2 symmetric) have their mirror images (i.e. enantiomers) among the ΛΛ. The second subgroup ΔΛ consists of 16 different stereoisomers (each ΔΛ being identical to a ΛΔ) which include six pairs of enantiomers and four *meso* species.
[15] M. F. DaCruz, M. Zimmer, *Inorg. Chem.* **1996**, *35*, 2872–2877.
[16] 136 with the same torsional sense ΔΔ and 136 having opposite torsional sense ΔΛ.
[17] Insight II 3.0.0 and Discover 3.0.0, MSI, San Diego, **1995**.
[18] G. M. Sheldrick, *SHELX93, Program for Crystal Structure Refinement*, Universität Göttingen, **1993**; G. M. Sheldrick, *SHELXS-86, Program for Crystal Structure Solution*, Universität Göttingen, **1986**.

[96232]